Title: Patterns of microbiome variation among infrapopulations of permanent bloodsucking parasites

Authors: Jorge Doña[1, 2]*, Stephany Virrueta Herrera[1], Tommi Nyman[3], Mervi Kunnasranta[4,5], and Kevin P. Johnson[1]*

Author details:

[1]Illinois Natural History Survey, Prairie Research Institute, University of Illinois at Urbana-Champaign, 1816 S. Oak St., Champaign, Illinois 61820, USA.

[2]Departamento de Biología Animal, Universidad de Granada, Granada, 18001, Spain.

[3]Department of Ecosystems in the Barents Region, Norwegian Institute of Bioeconomy Research, Svanhovd 35, 9925 Svanvik, Norway.

[4]Department of Environmental and Biological Sciences, University of Eastern Finland, Yliopistokatu 7, 80101 Joensuu, Finland.

[5]Natural Resources Institute Finland, Joensuu, Finland.

Email addresses: Jorge Doña: jorged@illinois.edu; Stephany Virrueta Herrera: svirru2@illinois.edu; Tommi Nyman: tommi.nyman@nibio.no; Mervi Kunnasranta: mervi.kunnasranta@uef.fi; Kevin P. Johnson: kdpjohnso@illinois.edu

*Correspondence to: jorged@illinois.edu, kpjohnso@illinois.edu.

Abstract:

While interspecific variation in microbiome composition can often be readily explained by factors such as host species identity, there is still limited knowledge of how microbiomes vary at scales lower than the species level (e.g., between individuals or populations). Here, we evaluated variation in microbiome composition of individual parasites among infrapopulations (i.e., populations of parasites of the same species living on a single host individual). To address this question, we used genome-resolved and shotgun metagenomic data of 17 infrapopulations (balanced design) of the permanent, bloodsucking seal louse *Echinophthirius horridus* sampled from individual Saimaa ringed seals *Pusa hispida saimensis*. Both genome-resolved metagenomic and metagenomic classification approaches consistently show that parasite infrapopulation identity is a significant factor that explains both qualitative and quantitative patterns of microbiome variation at the intraspecific level. This study contributes to the general understanding of the factors driving patterns of intraspecific variation in microbiome composition, especially of bloodsucking parasites, and has implications for understanding how well-known processes occurring at higher taxonomic levels, such as phylosymbiosis, might arise in these systems.

Keywords: *genome-resolved metagenomics, host-symbiont, intraspecific variation, lice, microbiota, shotgun metagenomics, symbiont.*

41 **Introduction**

42 Patterns of inter- and intraspecific variation in microbiome composition of animals have received
43 much attention because the microbiome may influence many biological processes that have
44 considerable effects on the host (Clemente et al. 2012; Le Chatelier et al. 2013; Rothschild et al.
45 2018; Rudman et al. 2019; Velazquez et al. 2019). For instance, particular microbiome
46 compositions have been found to drive genomic adaptation (Rudman et al. 2019) or to confer
47 protection against pathogens (Velazquez et al. 2019).

48 In general, both stochastic (e.g., dispersal, or ecological drift) and deterministic (e.g., host
49 immunological regulation, or microbe–microbe interactions) processes operate across multiple
50 spatial scales to shape the composition of animal microbiomes (Adair and Douglas 2017; Kohl
51 2020). In particular, among the many determinants shaping microbiome composition, host species
52 identity has been repeatedly identified as a key factor determining the composition of animal
53 microbiomes (Brooks et al. 2016; Mazel et al. 2018; Nishida and Ochman 2018; Lutz et al. 2019;
54 Knowles et al. 2019; Lim and Bordenstein 2020; Song et al. 2020). In other words, microbiomes
55 of individuals of the same species tend to be more similar than to those of another species. This
56 pattern is generally the result of filtering microbial taxa by the host (e.g., through host diet, habitat,
57 or immune system, Adair and Douglas 2017) or result from host-microbe coevolution (Lim and
58 Bordenstein 2020). When this process exhibits phylogenetic signal, the pattern is known as
59 phylosymbiosis (i.e., microbial community relationships that recapitulate the phylogeny of their
60 host, Brucker and Bordenstein 2013; Brooks et al. 2016; Lim and Bordenstein 2020). Nonetheless,
61 several aspects of the variation of animal microbiomes are yet to be better understood (Lim and
62 Bordenstein 2020). In particular, for non-human animals, there is still much to learn about how
63 microbiomes vary at scales below the species level, such as between populations (Blekhman et al.

64 2015; Kohl et al. 2018; Rothschild et al. 2018; Campbell et al. 2020; Fountain-Jones et al. 2020)

65 or ecotypes (Agany et al. 2020).

66 An area of focus on understanding intraspecific variation in microbiome composition has been
67 bloodsucking parasites. In these parasites, previous studies have consistently found a major role
68 of the host species in shaping microbiome composition in the parasites (Osei-Poku et al. 2012;

69 Zhang et al. 2014; Swei and Kwan 2017; Zolnik et al. 2018; Landesman et al. 2019; Lee et al.
70 2019; Muturi et al. 2019). However, in ticks (*Ixodes scapularis*), host individual identity of the
71 blood meal was even more important than host species identity in explaining microbiome
72 composition (Landesman et al. 2019). These results suggested that individual host identity of the
73 blood meal might be an important factor that shapes parasite microbiomes at the intraspecific level
74 (Landesman et al. 2019). In theory, microbiomes of individual bloodsucking parasites could vary
75 due to: 1) the individual parasite immune system that may impose selection on different bacterial
76 taxa (Blekhman et al. 2015; Suzuki et al. 2019), 2) differences in the source of the blood meal that
77 may transfer or disperse particular bacterial taxa, or modulate bacteria by creating specific
78 conditions during digestion (Rothschild et al. 2018), 3) microbe–microbe interactions (Hassani et
79 al. 2018), and 4) stochastic processes (e.g., ecological drift) (Lankau et al. 2012). However, for
80 most species, and for bloodsucking parasites in particular, the nature of intraspecific variation in
81 microbiomes and the relative importance of factors shaping this variation remain understudied.

82 Sucking lice (Phthiraptera: Anoplura) are permanent blood-feeding ectoparasites that live in the
83 fur or hairs of mammals. The sucking lice of pinnipeds (seals, sea lions, and walrus) are of
84 particular interest because of their need to adapt to the aquatic lifestyle of their hosts (Durden and
85 Musser 1994; Leonardi et al. 2013). There is evidence that the sucking of lice of seals and sea

86 lions have codiversified with their hosts (Kim 1971, 1975, 1985; Leonardi et al. 2019). In addition,
87 the sucking lice of pinnipeds represent an interesting system in which to study the variation in
88 microbiome composition and the drivers of this variation at an intraspecific level because: 1) these
89 lice have well defined, isolated populations (infrapopulations) on individual seal hosts, due to an
90 expected low rate of horizontal dispersal among host individuals, which is only possible during
91 the seals' haul-out periods on land or ice (Kim 1985; Leonardi et al. 2013, 2019); and 2) these lice
92 feed only upon the blood of their host (Snodgrass 1944; Kim 1985), so that it can be assumed that
93 individuals from the same infrapopulation feed upon "exactly" the same resource (i.e., the blood
94 of the individual seal on which they occur).

95 Here, we used genome-resolved approaches (the construction of draft microbial genomes from
96 short-read shotgun sequencing data; Bowers et al. 2017; Uritskiy et al. 2018) and metagenomic
97 classification tools (taxonomic classification of individual sequencing reads; Menzel et al. 2016)
98 to infer patterns of microbiome variation among individuals of the sucking seal louse
99 *Echinophthirius horridus* (von Olfers, 1816) inhabiting individual Saimaa ringed seals *Pusa*
100 *hispida saimensis* (Nordquist, 1899). Our sampling design, involving analysis of two individual
101 lice from each of 17 seals, allowed us to evaluate the degree to which variation in microbiome
102 composition among individual lice is explained by the infrapopulation (the identity of the seal
103 host).

104 **Materials and Methods**

105 <u>Sampling, DNA extraction, and sequencing</u>

106 Thirty-four individual lice were sampled from 17 individual Saimaa ringed seals (*Pusa hispida*
107 *saimensis*), which is an endemic endangered landlocked subspecies of the ringed seal living in

108 freshwater Lake Saimaa in Finland (e.g., Nyman et al. 2014). Individual lice were collected from
109 seals found dead or from seals that were live-captured for telemetry studies (e.g., Niemi et al.
110 2019), and placed in 2-ml screw-cap tubes with 99.5% ethanol. Lice from a single seal individual
111 were put in the same tube. Prior to DNA extraction, each louse individual was rinsed with 95 %
112 ethanol and placed alone in a new sterile vial; then, the remaining ethanol was evaporated at room
113 temperature.

114 Whole lice were ground up individually, and genomic DNA was extracted using the Qiagen
115 QIAamp DNA Micro Kit (Qiagen, Valencia, CA, U.S.A.). The standard protocol was modified
116 so that specimens were incubated in ATL buffer and proteinase K at 55 (insert degree) C for 48 h
117 instead of the recommended 1 – 3 h, as well as by substituting buffer AE with buffer EB (elution
118 buffer). This was done to ensure maximal yield (greater than 5 ng) of DNA from each louse. Each
119 DNA extract was quantified with a Qubit 2.0 Fluorometer (Invitrogen, Carlsbad, CA, U.S.A.)
120 following the manufacturer's recommended protocols.

121 Shotgun genomic libraries were prepared from the extracts with Hyper Library construction kits
122 (Kapa Biosystems, Wilmington, MA, U.S.A.), and the libraries were quantitated by qPCR and 150
123 bp pair-end sequenced on one lane of a NovaSeq 6000 sequencer (Albany, New York). FASTQ
124 files from sequence data were generated and demultiplexed with bcl2fastq v.2.20. All library
125 preparations, sequencing, and FASTQ file generation were carried out at the W.M. Keck Center
126 (University of Illinois, Urbana, IL, U.S.A.). Raw reads were subsequently deposited to the NCBI
127 GenBank SRA database (Table S1).

128 <u>Metagenomic analyses</u>

129

130 For the genome-resolved metagenomic analyses, we used the metaWRAP v1.1.5 pipeline (Uritskiy
131 et al. 2018) along with all the recommended databases (i.e., Checkm_DB, NCBI_nt, and
132 NCBI_tax). We used the metaWRAP Read_qc module with default parameters to quality trim the
133 reads and to de-contaminate each sample from host reads. For decontamination, we ran a de-novo
134 genome assembly of an individual louse of the same species, not included in this study, and with
135 a high amount of sequencing data ("Echor52") in Abyss v2.0.1 (Jackman et al. 2017). Finally, we
136 filtered out all non-bacterial reads from the contig file using Blobtools v1.0.1 (Laetsch and Blaxter
137 2017) and used this file to decontaminate all the other samples with the metaWRAP Read_qc
138 module. Next, we co-assembled reads from all the samples with the metaWRAP Assembly
139 module (--usemetaspades option) (Nurk et al. 2017). For this assembly, and because of memory
140 limitations, we used BBNorm (sourceforge.net/projects/bbmap/) before assembly to reduce the
141 coverage of the concatenated FASTQ file to a maximum of 100X and to discard reads with
142 coverage under 3X. We binned reads with the metaWRAP Binning module (--maxbin2 --concoct
143 --metabat2 options) (Alneberg et al. 2014; Wu et al. 2016; Kang et al. 2019) and then consolidated
144 the resulting bins into a final bin set with both metaWRAP's Bin_refinement module (-c 50 -x 10
145 options) and the Reassemble_bins module. We quantified the bins resulting from the
146 Bin_refinement module with Salmon (Patro et al. 2017) using the Quant_bins module with default
147 parameters. Finally, we classified bins using the Classify_bins module. This module uses Taxator-
148 tk, which gives highly accurate but conservative classifications (Dröge et al. 2015). Accordingly,
149 we also uploaded our final metagenome-assembled genomes (MAGs) to MiGA for a
150 complementary analysis to determine the most likely taxonomic classification and novelty rank of
151 the bin (Rodriguez-R et al. 2018). We used the NCBI Genome database (Prokaryotes; February
152 26, 2020 version) for this analysis.

153 For the metagenomic classification of reads, we used the metagenomic classifier Kaiju (Menzel et
154 al. 2016) with Reference database: nr (Bacteria and Archaea; Database date: 2017-05-16). We
155 used the default parameters for these analyses – SEG low complexity filter: yes; Run mode:
156 greedy; Minimum match length: 11; Minimum match score: 75; Allowed mismatches: 5. We then
157 converted Kaiju's output files into a summary table at the genus and species level and filtered out
158 taxa with low abundances (<0.1 % of the total reads). We also removed poorly identified taxa
159 because they would artificially increase the similarity between our samples. Specifically, the
160 following taxa were excluded: "NA", "Viruses", "archaeon", "uncultured bacterium", "uncultured
161 Gammaproteobacteria bacterium" (Table S2 and S3).

162 Lastly, we used Decontam v1.2.1 to filter out bacterial taxa exhibiting known statistical properties
163 of contaminants (Davis et al. 2018). We used the frequency method (*isContaminant* function)
164 which is based on the inverse relationship between the relative abundance of contaminants and
165 sample DNA concentration, and also has been found suitable for samples dominated by host DNA
166 (Willner et al. 2012; Lusk 2014; Salter et al. 2014; Jervis-Bardy et al. 2015; Hooper et al. 2019;
167 McArdle and Kaforou 2020). As input for Decontam analyses, we used the aforementioned total
168 DNA concentration values. Then, as recommended, we explored the distribution of scores
169 assigned by Decontam to assign the threshold according to bimodality between very low and high
170 scores (Davis et al. 2018). For the MAGs matrix, no bimodality was found, and thus we used the
171 0.1 default value (Fig S1a). None of the MAGs were classified as contaminants, according to
172 Decontam. For Kaiju matrices, a 0.3 threshold value was selected for the species matrix (Fig S1b)
173 and 0.31 for the genus matrix (Fig S1c). Decontam filtered out a single species (*Clostridia*
174 bacterium k32) from the species matrix and two genera (*Cupriavidus* and *Massilia*) from the genus
175 matrix.

176 Statistical analyses

177 To visualize similarities of microbiome composition among louse individuals from the same or
178 different individual seal hosts, we constructed non-metric multidimensional scaling (NMDS)
179 ordinations based on Bray–Curtis and Jaccard (binary = T) dissimilarities using the phyloseq
180 v1.26-1 R package (McMurdie and Holmes 2013). For the genome-resolved metagenomic
181 analyses, we used the normalized MAGs compositional matrices resulting from Salmon.
182 Specifically, these MAG counts are standardized to the individual sample size (MAG copies per
183 million reads) and thus allow between-sample comparisons. For the Kaiju analyses, we used the
184 rarefy_even_depth function of phyloseq (without replacement as in the hypergeometric model) to
185 rarefy samples to the smallest number of classified sequences per individual observed (85,513, and
186 71,267 reads in genus and species matrices, respectively) (Weiss et al. 2017). To assess the
187 influence of individual host identity on the microbiome composition of louse individuals, we
188 conducted a permutational multivariate analysis of variance (PERMANOVA) (Anderson and
189 Walsh 2013; Anderson 2014). PERMANOVA analyses were done using the *adonis2* function in
190 vegan v2.5–4 (Oksanen et al. 2019), based on Bray–Curtis and Jaccard distance matrices with 100
191 iterations. In PERMANOVA analyses, for the individual host identity factor, our within-group
192 sample size (n=2) was smaller than both the total number of groups (n=17) and the total sample
193 size (n=34). Thus, to account for a potential deviation in F-statistics and R^2 values (Kelly et al.
194 2015), we wrote an R simulation that randomly subsampled the infrapopulations from which the
195 louse came (5 infrapopulations per iteration). We ran 10 iterations and ran a PERMANOVA
196 analysis for each iteration. Note that, for a few iterations, subsampled samples were too similar
197 and PERMANOVA could not be done. In addition, we ran PERMANOVA analyses to explore
198 additional factors (louse sex: male, female; sequencing lane: 1, 2; and host status: dead, alive) that

199 may explain variance in microbiome composition. Furthermore, we included significant factors
200 as the first factors of the host identity PERMANOVA models (i.e., to obtain the variance explained
201 by host identity after accounting for the variance explained by that factor). We also restricted the
202 groups in which permutations could be done to only those with the same value of that vector using
203 the strata argument (e.g., for a sample collected from a dead host, and for the host-status factor,
204 permutations could only be done among other dead hosts). Lastly, we ran a Mantel test using the
205 *mantel* function in vegan (method=spearman, permutations=9999) to explore if host locality (i.e.,
206 the coordinates in which each host was sampled) correlated with the microbiome composition of
207 louse individuals. For this analysis, we ran 10 iterations of an R simulation in which we randomly
208 subsampled one louse sample for each individual host and ran a Mantel test for each iteration. The
209 following packages were used to produce the plots: ggplot2 v3.1.0.9 (Wickham 2016), grid v3.5.3
210 (R Core Team 2019), gridExtra v.2.3 (Auguie 2016), ggrepel v0.8.0 (Slowikowski et al. 2019),
211 ggpubr v.0.2.5 (Kassambara 2018), and ggsci v2.9 (Xiao 2018).

212 **Results**

213 From the genome-resolved metagenomics pipeline, 13 high-quality bacterial metagenome-
214 assembled genomes (MAGs) were obtained (Table 1; Fig 1). According to MiGA analyses, 10 of
215 them (77%) likely belong to a species not represented in the NCBI Genome database.

216 Kaiju analyses recovered a higher diversity of microorganisms than did the genome-resolved
217 approach. These differences are likely because of the quality-filtering parameters used in the
218 genome-resolved metagenomics pipeline (i.e., these taxa may have been discarded because the
219 completeness values of their bins were lower than 50% and/or their contamination values were
220 higher than 10%). Nevertheless, bacterial taxa found in the genome-resolved metagenomic

221 approach were generally found also in Kaiju and with similar relative abundances (Fig 2), and a
222 similar pattern was found also at the species level (Fig S2).

223 Ordination and PERMANOVA analyses show a major role of infrapopulation identity in
224 explaining microbiome composition for both presence–absence and quantitative data. In the
225 genome-resolved metagenomic dissimilarity matrices, most (>84% in all cases) of the variance
226 was explained by infrapopulation identity (PERMANOVA: Bray-Curtis, R^2= 0.857, F=6.419,
227 P=0.001, Fig 3a; Jaccard, R^2= 0.842, F= 5.671, P=0.001; Fig S3a). Results from the simulations
228 were in line with the results of the regular model, and thus support that our results were not biased
229 by the sampling design [PERMANOVA: Bray-Curtis, R^2 (min= 0.65, max= 0.98, mean= 0.78); P
230 (min= 0.001, max= 0.019, n<0.05= 10/10); Jaccard, R^2 (min= 0.66, max= 1, mean= 0.86), P (min=
231 0.001, max= 0.106, n<0.05= 5/7)]. From all the additional factors examined, only host status (i.e.,
232 dead, alive) explained a significant amount of variance [PERMANOVA: Bray-Curtis, Host status:
233 R^2= 0.28, F= 12.72, P= 0.001, Louse sex: R^2= 0.08, F= 0.9, P= 0.554, Sequencing lane: R^2= 0.01,
234 F= 0.38, P= 0.878; Jaccard, Host status: R^2= 0.13, F= 4.93, P= 0.002, Louse sex: R^2= 0.03, F=
235 0.28, P= 0.867, Sequencing lane: R^2= 0, F= -0.01, P= 1; Mantel test, locality, Bray-Curtis: ρ (min=
236 -0.09, max= -0.09, mean= -0.09), P (min= 0.8749, max= 0.8867, n<0.05= 0/10); Jaccard: ρ (min=
237 -0.29, max= -0.29, mean= -0.29), P (min= 0.97742, max= 0.9777, n<0.05= 0/10)]. Including host
238 status in PERMANOVA analyses did not alter the results on the major influence of host identity
239 in explaining microbiome composition (PERMANOVA: Host identity, Bray-Curtis, R^2= 0.57, F=
240 4.58, P= 0.001; Jaccard, R^2= 0.71, F= 5.09, P= 0.002).

241 Similarly, in Kaiju matrices collapsed at the species level, most (>80% in all cases) of the variance
242 was also explained by infrapopulation identity (PERMANOVA: Bray–Curtis, R^2=0.804, F=4.346,
243 P=0.001, Fig 3b; Jaccard, R^2=0.803, F=4.319, P=0.001; Fig S3b). Again, results from simulations

244 were similar [PERMANOVA: Bray-Curtis, R^2 (min= 0.62, max= 0.88, mean= 0.75); P (min=
245 0.003, max= 0.058, n<0.05= 9/10); Jaccard, R^2 (min= 0.63, max= 0.95, mean= 0.76), P (min=
246 0.002, max= 0.09, n<0.05= 9/10)]. Of all the others factors examined, only host status explained
247 a significant amount of variance [PERMANOVA: Bray-Curtis, Host-status: R^2= 0.22, F= 9.03, P=
248 0.001, Louse sex: R^2= 0.08, F= 0.81, P= 0.564, Sequencing lane: R^2= 0.01, F= 0.35, P= 0.859;
249 Jaccard, Host-status: R^2= 0.21, F= 8.73, P= 0.001, Louse sex: R^2= 0.08, F= 0.88, P= 0.497,
250 Sequencing lane: R^2= 0.01, F= 0.4, P= 0.825; Mantel test, locality, Bray-Curtis: ρ (min= 0.04,
251 max= 0.04, mean= 0.04), P (min= 0.5637, max= 0.5785, n<0.05= 0/10); Jaccard: ρ (min= -0.03,
252 max= -0.03, mean= -0.03), P (min= 0.5337, max= 0.5488, n<0.05= 0/10)]. PERMANOVA
253 analysis accounting for host status did not alter the significance of host identity (PERMANOVA:
254 Bray-Curtis, R^2= 0.52, F= 1.78, P= 0.007; Jaccard, R^2= 0.59, F= 3.37, P= 0.001).

255 Furthermore, results were consistent when using matrices collapsed at the genus level (>77% of
256 variance explained in all cases) (PERMANOVA: Bray–Curtis, R^2= 0.865, F= 6.804, P= 0.001, Fig
257 S4a; Jaccard, R^2= 0.774, F= 3.634, P= 0.001; Fig S4b). Once again, results from simulations were
258 similar [PERMANOVA: Bray-Curtis, R^2 (min= 0.68, max= 0.96, mean= 0.8); P (min= 0.002,
259 max= 0.073, n<0.05= 9/10); Jaccard, R^2 (min= 0.54, max= 0.86, mean= 0.73), P (min= 0.003,
260 max= 0.061, n<0.05= 9/10)]. Additionally, of all the others factors examined, only host status
261 explained a significant amount of variance [PERMANOVA: Bray-Curtis, Host-status: R^2= 0.3, F=
262 14, P= 0.001, Louse sex: R^2= 0.05, F= 0.51, P= 0.851, Sequencing lane: R^2= 0.01, F= 0.39, P=
263 0.753; Jaccard, Host-status: R^2= 0.18, F= 7.19, P= 0.002, Louse sex: R^2= 0.07, F= 0.75, P= 0.53,
264 Sequencing lane: R^2= 0.01, F= 0.40, P= 0.75; Mantel test, locality, Bray-Curtis: ρ (min= 0.09,
265 max= 0.09, mean= 0.09), P (min= 0.7198, max= 0.7344, n<0.05= 0/10); Jaccard: ρ (min= 0.02,
266 max= 0.02, mean= 0.02), P (min= 0.4043, max= 0.4246, n<0.05= 0/10)]. Likewise,

267 PERMANOVA analysis accounting for host status did not alter the significance of host identity
268 (PERMANOVA: Bray-Curtis, R^2= 0.56, F= 4.73, P= 0.001; Jaccard, R^2= 0.59, F= 2.96, P= 0.001).

269 **Discussion**

270 Two different metagenomic approaches support a major role of infrapopulation identity (ringed
271 seal host individual) in explaining microbiome variation among individuals of the seal louse. In
272 addition, highly similar results were found for approaches using either presence-absence or
273 quantitative matrices, suggesting that not only is bacterial composition, but also bacterial
274 abundance explained by infrapopulation identity. Our analyses were done on whole louse
275 individuals and, thus, we cannot confidently differentiate between bacterial taxa inhabiting the lice
276 (e.g., *Wolbachia* or *Hodgkinia*) from transient taxa present in the host blood meal (e.g.,
277 *Chlamydia*). Nevertheless, in line with current evidence on the determinants of microbiome
278 composition of bloodsucking parasites, the louse blood meal from individual seals is the most
279 likely candidate in explaining the patterns of microbiome variation across the louse
280 infrapopulations found here. Indeed, many of the taxa found in our analyses have already been
281 found in other bloodsucking parasites, thus supporting the influence of blood in shaping the
282 composition of parasite microbiomes studied here (Jiménez-Cortés et al. 2018).

283 However, other factors in addition to blood may have contributed to the similarity of microbiomes
284 between individual lice from the same seal host individual. Some similarity may have arisen from
285 shared environmental bacteria, those on the surface of the louse from a shared environment (skin
286 and fur of the host), or contamination between louse individuals in screw-cap tubes, and not filtered
287 by our decontamination procedures. There may also be insect-specific bacterial taxa, independent
288 from the host blood, that are shared horizontally between individual lice from the same
289 infrapopulation. Finally, louse infrapopulations are known to typically be highly inbred, with a

290 high level of relatedness between individuals (Koop et al. 2014, DiBlasi et al 2018, Virrueta
291 Herrera et al., in prep.). It may be that there are louse genetic factors that interact with the
292 microbiome to produce a specific composition (Blekhman et al. 2015; Dobson et al. 2015; Suzuki
293 et al. 2019).

294 Our results are congruent with previous findings on the influence of host blood on microbiomes
295 of bloodsucking parasites. Specifically, several studies have found a major role of the specific
296 host species from which a blood meal is taken in shaping microbiomes of other bloodsucking
297 organisms, such as ticks (*Ixodes scapularis, Ixodes pacificus*) and mosquitoes (*Aedes aegypti*)
298 (Swei and Kwan 2017; Landesman et al. 2019; Muturi et al. 2019). Furthermore, Landesman et
299 al. (2019) showed that microbiomes of deer tick (*Ixodes scapularis*) nymphs were largely
300 explained by the individual hosts of the tick, a result similar to the one obtained here. Interestingly,
301 in that study, the percentage of variation explained was considerably lower (45%) than that found
302 here (>77%). It may be that differences in parasite ecology, such as the whether the parasite is a
303 permanent or a recurrent feeder (as are both the case in sucking lice) may modulate the extent to
304 which host blood shapes parasite microbiomes. The differences in the proportion of variance
305 explained by infrapopulation identity between the two studies could also be due to differences in
306 experimental design, such as the number of sampled infrapopulations (3 in ticks, and 17 in the seal
307 lice here) and whether the sample design is balanced (i.e., the same number of individual parasites
308 sampled per infrapopulation).

309 The knowledge that blood from the same individual seal host may influence the similarity of the
310 microbiome of blood-feeding lice from that host can potentially provide new insights into the
311 influence of host blood on such parasites. There are least two not necessarily mutually exclusive
312 processes may explain the influence of a host individual's blood on louse microbiomes. First, the

313 blood from a particular host individual may contain a specific composition of bacterial loads that
314 enter the louse on consumption of blood. Indeed, anopluran lice might have a higher likelihood
315 of being colonized by bacteria from host blood because they do not possess a peritrophic
316 membrane, an extracellular layer in the midgut that is composed of chitin, proteoglycans, and
317 proteins, which in most other insects surrounds the ingested food bolus and separates the gut
318 content, including bacteria, from the epithelium (Terra 2001; Waniek 2009). Indeed, the idea that
319 a lack of a peritrophic membrane may facilitate colonization of blood-feeding parasites by bacteria
320 present in the host blood has potentially also been supported by work on mouse fleas
321 (*Rhadinopsylla dahurica*), which also lack this membrane (Li et al. 2018). In this case, there was
322 evidence of homogenization (i.e., similar bacterial communities) between the host blood and the
323 parasite (whole flea individuals). The lack of a peritrophic membrane is often associated with
324 permanent parasites, such as blood-feeding lice, for which the continual availability of food means
325 that there is less selection for efficiency of digestion. Therefore, the presence versus absence of a
326 peritrophic membrane may explain the differences between lice and ticks (of which the latter
327 possess a peritrophic membrane) with regards to the influence of host blood on the composition of
328 the parasite microbiome.

329 A second possibility that could explain why host blood may influence louse microbiome
330 composition is that the conditions during blood digestion may alter bacterial taxa that were already
331 present in the louse. The specifics of blood digestion may have an individual host-specific
332 signature. Specifically, catabolism of blood meal leads to the generation of reactive oxygen
333 species that are known to alter the midgut bacterial composition and diversity of bloodsucking
334 parasites (Souza et al. 1997; Wang et al. 2011; Muturi et al. 2019). Also, the blood meals of
335 different host species are also known to differ in composition (e.g., total protein, hemoglobin, and

336 hematocrit content), and these differences may lead to a differential proliferation of microbial taxa
337 during digestion by the parasite (Souza et al. 1997; Wang et al. 2011; Muturi et al. 2019). It may
338 be the case that differences in blood composition among individuals even within the same host
339 species may be shaping the bacterial composition of lice in a manner that is specific to host
340 individuals.

341 Bloodsucking organisms, and anopluran lice in particular, are well known to rely on mutualistic
342 endosymbionts to complement deficiencies in their diet (Perotti et al. 2008; Boyd and Reed 2012;
343 Boyd et al. 2017; Jiménez-Cortés et al. 2018). Notwithstanding that several of the bacterial taxa
344 we found may not be stable inhabitants of lice, we did find evidence for the presence of several
345 louse-specific bacterial taxa. These include the obligate intracellular arthropod bacteria *Wolbachia*
346 (Werren 1997) and *Hodgkinia* (for which only endosymbionts of *Cicadas* are known; McCutcheon
347 et al. 2009). Accordingly, we explored our MAGs for genome characteristics typical of
348 endosymbionts. In particular, because endosymbiont genomes typically are small and have an AT
349 bias, we explored the relative position of the observed MAGs in a "Genome size ~ GC content"
350 correlation plot (Wernegreen 2015; Figure 4). Bin 1 appears to be the best candidate to be a
351 mutualistic endosymbiont, according to its relative position in the correlation plot. This MAG was
352 100% complete (according to CheckM; Parks et al. 2015), detected in most samples (prevalence =
353 71%), and classified with confidence as Flavobacteriaceae. MiGA analyses suggest it may even
354 belong to *Chryseobacterium* (p-value 0.585). Endosymbionts belonging to *Chryseobacterium* are
355 known in other arthropods (e.g., termites, mosquitoes, cockroaches, and ticks; Eutick et al. 1978;
356 Dugas et al. 2001; Campbell et al. 2004; Montasser 2005; Burešová et al. 2006). Additionally, we
357 conducted a preliminary investigation of the metabolic capabilities of this bacterium by
358 investigating the completeness of metabolic pathways using GhostKOALA (Kanehisa et al. 2016)

359 and KEGG-Decoder (Graham et al. 2018). This MAG has complete routes for synthesis of vitamin
360 B (riboflavin), an essential amino acid (lysine), and several non-essential amino acids (e.g., serine;
361 see Table S4), as well as many fully or partially missing routes that may be redundant or potentially
362 shared (or synthesized along) with the louse (Table S4).

363 Overall, these results are congruent with what has been found for endosymbionts of bloodsucking
364 parasites (Moriyama et al. 2015; Boyd et al. 2016; Santos-Garcia et al. 2017; Duron et al. 2018).
365 Another anopluran pinniped louse (*Proechinophthirus fluctus*) has been found to have a *Sodalis*
366 endosymbiont (Boyd et al. 2016), but we found no evidence of *Sodalis* in *Echinophthirius*
367 *horridus*. Other species of Anoplura have yet other endosymbionts (Boyd et al. 2017, Ríhová et
368 al. 2017), suggesting that endosymbiont replacement is an ongoing and relatively common process
369 within the order. Further research, including phylogenomic studies improving the phylogenetic
370 placement of this potentially mutualistic bacterium and studies using fluorescence in situ
371 hybridization (FISH) to ascertain the location of this bacterium in louse individuals, is needed to
372 get deeper insight into the interaction of this bacterium with *E. horridus*.

373 Finally, at a broader scale, our results are congruent with previous studies that have found a major
374 role of different levels of subdivision in shaping microbiomes in a wide range of systems. For
375 instance, population identity has been found to largely explain microbiome composition of great
376 apes (Campbell et al. 2020), American pikas (*Ochotona princeps*) (Kohl et al. 2018), and humans
377 (Rothschild et al. 2018). Similar results have also been found across subdivision levels other than
378 populations, such as ecotypes (human lice *Pediculus humanus*; Agany et al. 2020), or by spatial
379 proximity (North American moose *Alces alces*; Fountain-Jones et al. 2020). On the other hand,
380 while the influence of subdivision on microbiome composition is widely supported, much less is
381 known about whether signs of phylosymbiosis can be found at these levels. Kohl et al. (2018)

382 found that populations largely explained microbiome variation in American pikas along with a
383 phylosymbiotic pattern (i.e., closely related hosts had similar microbial communities).
384 Interestingly, while we did not investigate the presence of phylosymbiosis here, our results suggest
385 that a phylosymbiotic pattern is not always found at an intraspecific level. For instance, this may
386 be the case of subdivided systems in which the food source (which allows the dispersal of microbes
387 from one organism to another) constitutes the main determinant of microbiome composition, and
388 populations are not necessarily composed of closely related organisms. However, phylosymbiotic
389 patterns across species have been found in relatively similar systems. Therefore, bacterial
390 dispersal, ecological drift, diversification, or microbe-microbe interactions may be the main factors
391 explaining phylosymbiosis in these systems. More studies on the origin and prevalence of
392 phylosymbiotic patterns within and across species are clearly needed.

393

394 **Acknowledgments:** We thank seal researchers and students for collecting the lice analyzed in
395 this study.

396 **Author contributions:** J.D., S.V.H, and K.P.J. conceived the study. T.N. and M.K. obtained
397 samples. S.V.H. and K.P.J. collected the data. J.D. analyzed the data. T.N., M.V., and K.P.J.
398 obtained financial support for the project. J.D. wrote the manuscript and all authors contributed
399 to editing the manuscript.

400 **Funding:** This study was supported by the US National Science Foundation (DEB-1239788 and
401 DEB-1342604 to K.P.J). Sequencing costs were supported by grants from the Oskar Öflund
402 Foundation, the Betty Väänänen Foundation, Societas Pro Fauna et Flora Fennica, and the
403 Nestori Foundation.

404 **Availability of data and material:** Raw sequence reads for all samples are available under
405 (NCBI) project *ACCESSION CODE*. Metagenomic assemblies are available at Figshare (doi:
406 10.6084/m9.figshare.12366575 —private link for review:
407 https://figshare.com/s/171207f7fb73f7d290a6). Metagenomic assemblies are also available from
408 NCBI Genome (*ACCESION CODES*).

409 **Ethics approval and consent to participate:** Telemetry studies have been approved by the local
410 environmental authority Centre for Economic Development, Transport and the Environment
411 (permit numbers: ESAELY/433/ 07.01/2012 and ESA-2008-L-519-254) and the Animal
412 Experiment Board in Finland (permit numbers: ESAVI/ 8269/04.10.07/2013 and ESAVI-2010-
413 08380/Ym-23).

414 **Competing interests:** The authors declare that they have no competing interests.
415

416 **References:**

417 Adair, K. L., and A. E. Douglas. (2017). Making a microbiome: the many determinants of host-
418 associated microbial community composition. *Current Opinion in Microbiology*, 35, 23–
419 29.
420 Agany, D. D. M., R. Potts, J. L. Gonzalez Hernandez, E. Z. Gnimpieba, and J. E. Pietri. (2020).
421 Microbiome Differences between Human Head and Body Lice Ecotypes Revealed by
422 16S rRNA Gene Amplicon Sequencing. *Journal of Parasitology*, 106, 14.
423 Alneberg, J., B. S. Bjarnason, I. de Bruijn, M. Schirmer, J. Quick, U. Z. Ijaz, L. Lahti, N. J.
424 Loman, A. F. Andersson, and C. Quince. (2014). Binning metagenomic contigs by
425 coverage and composition. *Nature Methods*, 11, 1144–1146.
426 Anderson, M. J. (2014). Permutational multivariate analysis of variance (PERMANOVA). *Wiley*
427 *statsref: statistics reference online*, 1–15.
428 Anderson, M. J., and D. C. Walsh. (2013). PERMANOVA, ANOSIM, and the Mantel test in the
429 face of heterogeneous dispersions: what null hypothesis are you testing? *Ecological*
430 *Monographs*, 83, 557–574.
431 Auguie, B. (2016). gridExtra: Miscellaneous functions for "Grid" graphics. R package version
432 2.3. URL https://CRAN. R-project. org/package= gridExtra.
433 Blekhman, R., J. K. Goodrich, K. Huang, Q. Sun, R. Bukowski, J. T. Bell, T. D. Spector, A.
434 Keinan, R. E. Ley, D. Gevers, and A. G. Clark. (2015). Host genetic variation impacts
435 microbiome composition across human body sites. *Genome Biology*, 16, 191.
436 Bowers, R. M., N. C. Kyrpides, R. Stepanauskas, M. Harmon-Smith, D. Doud, T. B. K. Reddy,
437 F. Schulz, J. Jarett, A. R. Rivers, E. A. Eloe-Fadrosh, S. G. Tringe, N. N. Ivanova, A.
438 Copeland, A. Clum, E. D. Becraft, R. R. Malmstrom, B. Birren, M. Podar, P. Bork, G. M.
439 Weinstock, G. M. Garrity, J. A. Dodsworth, S. Yooseph, G. Sutton, F. O. Glöckner, J. A.
440 Gilbert, W. C. Nelson, S. J. Hallam, S. P. Jungbluth, T. J. G. Ettema, S. Tighe, K. T.
441 Konstantinidis, W.-T. Liu, B. J. Baker, T. Rattei, J. A. Eisen, B. Hedlund, K. D.
442 McMahon, N. Fierer, R. Knight, R. Finn, G. Cochrane, I. Karsch-Mizrachi, G. W. Tyson,
443 C. Rinke, A. Lapidus, F. Meyer, P. Yilmaz, D. H. Parks, A. M. Eren, L. Schriml, J. F.
444 Banfield, P. Hugenholtz, and T. Woyke. (2017). Minimum information about a single
445 amplified genome (MISAG) and a metagenome-assembled genome (MIMAG) of
446 bacteria and archaea. *Nature Biotechnology*, 35, 725–731.
447 Boyd, B. M., J. M. Allen, R. Koga, T. Fukatsu, A. D. Sweet, K. P. Johnson, and D. L. Reed.
448 (2016). Two Bacterial Genera, Sodalis and Rickettsia, Associated with the Seal Louse
449 Proechinophthirus fluctus (Phthiraptera: Anoplura). *Applied and Environmental*
450 *Microbiology*, 82, 3185–3197.
451 Boyd, B. M., J. M. Allen, N.-P. Nguyen, P. Vachaspati, Z. S. Quicksall, T. Warnow, L. Mugisha,
452 K. P. Johnson, and D. L. Reed. (2017). Primates, Lice and Bacteria: Speciation and
453 Genome Evolution in the Symbionts of Hominid Lice. *Molecular Biology and Evolution,*
454 34, 1743–1757.
455 Boyd, B. M., and D. L. Reed. (2012). Taxonomy of lice and their endosymbiotic bacteria in the
456 post-genomic era. *Clinical Microbiology and Infection*, 18, 324–331.
457 Brooks, A. W., K. D. Kohl, R. M. Brucker, E. J. van Opstal, and S. R. Bordenstein. (2016).
458 Phylosymbiosis: Relationships and Functional Effects of Microbial Communities across
459 Host Evolutionary History. *PLoS Biology*, 14, e2000225.
460 Brucker, R. M., and S. R. Bordenstein. (2013). The Hologenomic Basis of Speciation: Gut

461 Bacteria Cause Hybrid Lethality in the Genus Nasonia. *Science*, 341, 667–669.
462 Burešová, V., Z. Franta, and P. Kopáček. (2006). A comparison of Chryseobacterium
463 indologenes pathogenicity to the soft tick Ornithodoros moubata and hard tick Ixodes
464 ricinus. *Journal of Invertebrate Pathology*, 93, 96–104.
465 Campbell, C. L., D. L. Mummey, E. T. Schmidtmann, and W. C. Wilson. (2004). Culture-
466 independent analysis of midgut microbiota in the arbovirus vector Culicoides sonorensis
467 (Diptera: Ceratopogonidae). *Journal of Medical Entomology*, 41, 340–348.
468 Campbell, T. P., X. Sun, V. H. Patel, C. Sanz, D. Morgan, and G. Dantas. (2020). The
469 microbiome and resistome of chimpanzees, gorillas, and humans across host lifestyle and
470 geography. *ISME Journal*, 1–16.
471 Clemente, J. C., L. K. Ursell, L. W. Parfrey, and R. Knight. (2012). The impact of the gut
472 microbiota on human health: an integrative view. *Cell*, 148, 1258–1270.
473 Davis, N. M., D. M. Proctor, S. P. Holmes, D. A. Relman, and B. J. Callahan. (2018). Simple
474 statistical identification and removal of contaminant sequences in marker-gene and
475 metagenomics data. *Microbiome*, 6, 226.
476 Díaz-Sánchez, S., A. Estrada-Peña, A. Cabezas-Cruz, and J. de la Fuente. (2019). Evolutionary
477 Insights into the Tick Hologenome. *Trends in Parasitology*, 35, 725–737.
478 Dobson, A. J., J. M. Chaston, P. D. Newell, L. Donahue, S. L. Hermann, D. R. Sannino, S.
479 Westmiller, A. C.-N. Wong, A. G. Clark, and B. P. Lazzaro. (2015). Host genetic
480 determinants of microbiota-dependent nutrition revealed by genome-wide analysis of
481 Drosophila melanogaster. *Nature Communications*, 6, 1–9.
482 Dröge, J., I. Gregor, and A. C. McHardy. (2015). Taxator-tk: precise taxonomic assignment of
483 metagenomes by fast approximation of evolutionary neighborhoods. *Bioinformatics,* 31,
484 817–824.
485 Dugas, J. E., L. Zurek, B. J. Paster, B. A. Keddie, and E. R. Leadbetter. (2001). Isolation and
486 characterization of a Chryseobacterium strain from the gut of the American cockroach,
487 Periplaneta americana. *Archives of Microbiology*, 175, 259–262.
488 Durden, L. A., and G. G. Musser. (1994). The mammalian hosts of the sucking lice (Anoplura)
489 of the world: a host-parasite list. *Journal of Vector Ecology*, 19, 130–168.
490 Duron, O., O. Morel, V. Noël, M. Buysse, F. Binetruy, R. Lancelot, E. Loire, C. Ménard, O.
491 Bouchez, F. Vavre, and L. Vial. (2018). Tick-Bacteria Mutualism Depends on B Vitamin
492 Synthesis Pathways. *Current Biology*, 28, 1896-1902.e5.
493 Eutick, M. L., R. W. O'brien, and M. Slaytor. (1978). Bacteria from the gut of Australian
494 termites. *Applied and Environmental Microbiology*, 35, 823–828.
495 Fountain-Jones, N. M., N. J. Clark, A. C. Kinsley, M. Carstensen, J. Forester, T. J. Johnson, E.
496 A. Miller, S. Moore, T. M. Wolf, and M. E. Craft. (2020). Microbial associations and
497 spatial proximity predict North American moose (Alces alces) gastrointestinal
498 community composition. *Journal of Animal Ecology*, 89, 817–828.
499 Graham, E. D., J. F. Heidelberg, and B. J. Tully. (2018). Potential for primary productivity in a
500 globally-distributed bacterial phototroph. ISME Journal, 12, 1861–1866.
501 Hassani, M. A., P. Durán, and S. Hacquard. (2018). Microbial interactions within the plant
502 holobiont. *Microbiome*, 6, 58.
503 Hooper, R., J. C. Brealey, T. van der Valk, A. Alberdi, J. W. Durban, H. Fearnbach, K. M.
504 Robertson, R. W. Baird, M. B. Hanson, P. Wade, M. T. P. Gilbert, P. A. Morin, J. B. W.
505 Wolf, A. D. Foote, and K. Guschanski. (2019). Host-derived population genomics data
506 provides insights into bacterial and diatom composition of the killer whale skin.

Molecular Ecology, 28, 484–502.
Jackman, S. D., B. P. Vandervalk, H. Mohamadi, J. Chu, S. Yeo, S. A. Hammond, G. Jahesh, H. Khan, L. Coombe, R. L. Warren, and I. Birol. (2017). ABySS 2.0: resource-efficient assembly of large genomes using a Bloom filter. *Genome Research*, 27, 768–777.
Jervis-Bardy, J., L. E. Leong, S. Marri, R. J. Smith, J. M. Choo, H. C. Smith-Vaughan, E. Nosworthy, P. S. Morris, S. O'Leary, and G. B. Rogers. (2015). Deriving accurate microbiota profiles from human samples with low bacterial content through post-sequencing processing of Illumina MiSeq data. *Microbiome*, 3, 19. Springer.
Jiménez-Cortés, J. G., R. García-Contreras, M. I. Bucio-Torres, M. Cabrera-Bravo, A. Córdoba-Aguilar, G. Benelli, and P. M. Salazar-Schettino. (2018). Bacterial symbionts in human blood-feeding arthropods: Patterns, general mechanisms and effects of global ecological changes. *Acta Tropica*, 186, 69–101.
Kanehisa, M., Y. Sato, and K. Morishima. (2016). BlastKOALA and GhostKOALA: KEGG tools for functional characterization of genome and metagenome sequences. *Journal of Molecular Biology*, 428, 726–731.
Kang, D. D., F. Li, E. Kirton, A. Thomas, R. Egan, H. An, and Z. Wang. (2019). MetaBAT 2: an adaptive binning algorithm for robust and efficient genome reconstruction from metagenome assemblies. *PeerJ*, 7:e7359.
Kassambara, A. (2018). Package 'ggpubr':'ggplot2'based publication ready plots. Version 0.2. See https://rpkgs. datanovia. com/ggpubr/index. html.
Kelly, B. J., Gross, R., Bittinger, K., Sherrill-Mix, S., Lewis, J. D., Collman, R. G., ... & Li, H. (2015). Power and sample-size estimation for microbiome studies using pairwise distances and PERMANOVA. *Bioinformatics*, 31, 2461-2468.
Kim, K. C. (1985). Coevolution of Parasitic Arthropods and Mammals. Wiley.
Kim, K. C. (1975). Specific antiquity of the sucking lice and evolution of otariid seals. *Rapports et procès-verbaux des réunions*, 169, 544–549.
Kim, K. C. (1971). The Sucking Lice (Anoplura: Echinophthiriidae) of the Northern Fur Seal; Descriptions and Morphological Adaptation. *Annals of the Entomological Society of America*, 64, 280–292
Knowles, S. C. L., Eccles, R. M., & Baltrūnaitė, L. (2019). Species identity dominates over environment in shaping the microbiota of small mammals. *Ecology Letters*, 22, 826-837.
Kohl, K. D. (2020). Ecological and evolutionary mechanisms underlying patterns of phylosymbiosis in host-associated microbial communities. *Philosophical Transactions of the Royal Society of London B Biological Sciences*, 375, 20190251.
Kohl, K. D., J. Varner, J. L. Wilkening, and M. D. Dearing. (2018). Gut microbial communities of American pikas (*Ochotona princeps*): Evidence for phylosymbiosis and adaptations to novel diets. *Journal of Animal Ecology*, 87, 323–330.
Laetsch, D. R., and M. L. Blaxter. (2017). BlobTools: Interrogation of genome assemblies. *F1000Research*, 6, 1287.
Landesman, W. J., K. Mulder, B. F. Allan, L. A. Bashor, F. Keesing, K. LoGiudice, and R. S. Ostfeld. (2019). Potential effects of blood meal host on bacterial community composition in Ixodes scapularis nymphs. *Ticks and Tick-Borne Diseases*, 10, 523–527.
Lankau, E. W., P.-Y. Hong, and R. I. Mackie. (2012). Ecological drift and local exposures drive enteric bacterial community differences within species of Galapagos iguanas. *Molecular Ecology*, 21, 1779–1788.
Le Chatelier, E., T. Nielsen, J. Qin, E. Prifti, F. Hildebrand, G. Falony, M. Almeida, M.

553 Arumugam, J.-M. Batto, S. Kennedy, P. Leonard, J. Li, K. Burgdorf, N. Grarup, T.
554 Jørgensen, I. Brandslund, H. B. Nielsen, A. S. Juncker, M. Bertalan, F. Levenez, N. Pons,
555 S. Rasmussen, S. Sunagawa, J. Tap, S. Tims, E. G. Zoetendal, S. Brunak, K. Clément, J.
556 Doré, M. Kleerebezem, K. Kristiansen, P. Renault, T. Sicheritz-Ponten, W. M. de Vos, J.-
557 D. Zucker, J. Raes, T. Hansen, P. Bork, J. Wang, S. D. Ehrlich, and O. Pedersen. (2013).
558 Richness of human gut microbiome correlates with metabolic markers. *Nature*, 500, 541–
559 546.
560 Lee, S., J. Y. Kim, M. Yi, I.-Y. Lee, R. Fyumagwa, and T.-S. Yong. (2019). Comparative
561 microbiomes of ticks collected from a black rhino and its surrounding environment.
562 *International Journal of Parasitology Parasites and Wildlife*, 9, 239–243.
563 Leonardi, M. S., E. A. Crespo, J. A. Raga, and F. J. Aznar. (2013). Lousy mums: patterns of
564 vertical transmission of an amphibious louse. *Parasitology Research*, 112, 3315–3323.
565 Springer.
566 Leonardi, M. S., S. V. Herrera, A. Sweet, J. Negrete, and K. P. Johnson. (2019). Phylogenomic
567 analysis of seal lice reveals codivergence with their hosts. *Systematic Entomology*, 44,
568 699–708.
569 Li, H., T. Li, and J. Qu. (2018). Stochastic processes govern bacterial communities from the
570 blood of pikas and from their arthropod vectors. *FEMS Microbiology Ecology,* 94.
571 Lim, S. J., and S. R. Bordenstein. (2020). An introduction to phylosymbiosis. *Proceedings of the*
572 *Royal Society B: Biological Sciences*, 287, 20192900.
573 Lusk, R. W. (2014). Diverse and widespread contamination evident in the unmapped depths of
574 high throughput sequencing data. *PloS One,* 9.
575 Lutz, H. L., E. W. Jackson, P. W. Webala, W. S. Babyesiza, J. C. Kerbis Peterhans, T. C.
576 Demos, B. D. Patterson, and J. A. Gilbert. (2019). Ecology and Host Identity Outweigh
577 Evolutionary History in Shaping the Bat Microbiome. *mSystems,* 4.
578 Mazel, F., K. M. Davis, A. Loudon, W. K. Kwong, M. Groussin, and L. W. Parfrey. (2018). Is
579 Host Filtering the Main Driver of Phylosymbiosis across the Tree of Life? *mSystems,* 3.
580 McArdle, A. J., and M. Kaforou. (2020). Sensitivity of shotgun metagenomics to host DNA:
581 abundance estimates depend on bioinformatic tools and contamination is the main issue.
582 *Access Microbiology*, doi: 10.1099/acmi.0.000104.
583 McCutcheon, J. P., B. R. McDonald, and N. A. Moran. *2009*. Origin of an Alternative Genetic
584 Code in the Extremely Small and GC–Rich Genome of a Bacterial Symbiont. *PLoS*
585 *Genetics*, 5, e1000565.
586 McMurdie, P. J., and S. Holmes. (2013). phyloseq: an R package for reproducible interactive
587 analysis and graphics of microbiome census data. *PloS One,* 8.
588 Menzel, P., K. L. Ng, and A. Krogh. (2016). Fast and sensitive taxonomic classification for
589 metagenomics with Kaiju. *Nature Communications*, 7, 1–9.
590 Montasser, A. A. (2005). Gram-negative bacteria from the camel tick Hyalomma dromedarii
591 (Ixodidae) and the chicken tick Argas persicus (Argasidae) and their antibiotic
592 sensitivities. *Journal of the Egyptian Society of Parasitology*, 35, 95–106.
593 Moriyama, M., N. Nikoh, T. Hosokawa, and T. Fukatsu. (2015). Riboflavin Provisioning
594 Underlies Wolbachia's Fitness Contribution to Its Insect Host. *mBio,* 6.
595 Muturi, E. J., C. Dunlap, J. L. Ramirez, A. P. Rooney, and C.-H. Kim. (2019). Host blood-meal
596 source has a strong impact on gut microbiota of Aedes aegypti. *FEMS Microbiology*
597 *Ecology*, 95.

598 Niemi, M., Liukkonen, L., Koivuniemi, M., Auttila, M., Rautio, A., & Kunnasranta, M. (2019).
599 Winter behavior of Saimaa ringed seals: Non-overlapping core areas as indicators of
600 avoidance in breeding females. *PloS one*, 14, 1.
601 Nishida, A. H., and H. Ochman. (2018). Rates of gut microbiome divergence in mammals.
602 *Molecular Ecology*, 27, 1884–1897.
603 Nurk, S., D. Meleshko, A. Korobeynikov, and P. A. Pevzner. (2017). metaSPAdes: a new
604 versatile metagenomic assembler. *Genome Research*, 27, 824–834.
605 Nyman, T., Valtonen, M., Aspi, J., Ruokonen, M., Kunnasranta, M. & Palo, J. U. (2014).
606 Demographic histories and genetic diversities of Fennoscandian marine and landlocked
607 ringed seal subspecies. *Ecology and Evolution*, 4, 3420-3434.
608 Oksanen, J., F. G. Blanchet, R. Kindt, P. Legendre, R. B. O'hara, G. L. Simpson, P. Solymos, M.
609 H. H. Stevens, and H. Wagner. (2019). Vegan: community ecology package. R package
610 version 2.5-4.
611 Osei-Poku, J., C. M. Mbogo, W. J. Palmer, and F. M. Jiggins. (2012). Deep sequencing reveals
612 extensive variation in the gut microbiota of wild mosquitoes from Kenya. *Molecular*
613 *Ecology*, 21, 5138–5150.
614 Parks, D. H., M. Imelfort, C. T. Skennerton, P. Hugenholtz, and G. W. Tyson. (2015). CheckM:
615 assessing the quality of microbial genomes recovered from isolates, single cells, and
616 metagenomes. *Genome Research*, 25, 1043–1055.
617 Patro, R., G. Duggal, M. I. Love, R. A. Irizarry, and C. Kingsford. (2017). Salmon provides fast
618 and bias-aware quantification of transcript expression. *Nature Methods*, 14, 417.
619 Perotti, M. A., E. F. Kirkness, D. L. Reed, and H. R. Braig. (2008). Endosymbionts of lice. Pp.
620 223–238 *in* Insect Symbiosis, Volume 3. CRC Press.
621 R Core Team. (2019). R: A language and environment for statistical computing.
622 Rodriguez-R, L. M., S. Gunturu, W. T. Harvey, R. Rosselló-Mora, J. M. Tiedje, J. R. Cole, and
623 K. T. Konstantinidis. (2018). The Microbial Genomes Atlas (MiGA) webserver:
624 taxonomic and gene diversity analysis of Archaea and Bacteria at the whole genome
625 level. *Nucleic Acids Research*, 46, W282–W288.
626 Rothschild, D., O. Weissbrod, E. Barkan, A. Kurilshikov, T. Korem, D. Zeevi, P. I. Costea, A.
627 Godneva, I. N. Kalka, N. Bar, S. Shilo, D. Lador, A. V. Vila, N. Zmora, M. Pevsner-
628 Fischer, D. Israeli, N. Kosower, G. Malka, B. C. Wolf, T. Avnit-Sagi, M. Lotan-Pompan,
629 A. Weinberger, Z. Halpern, S. Carmi, J. Fu, C. Wijmenga, A. Zhernakova, E. Elinav, and
630 E. Segal. (2018) Environment dominates over host genetics in shaping human gut
631 microbiota. *Nature*, 555, 210–215.
632 Rudman, S. M., S. Greenblum, R. C. Hughes, S. Rajpurohit, O. Kiratli, D. B. Lowder, S. G.
633 Lemmon, D. A. Petrov, J. M. Chaston, and P. Schmidt. (2019). Microbiome composition
634 shapes rapid genomic adaptation of *Drosophila melanogaster*. *Proceedings of the*
635 *National Academy of Sciences USA*, 116, 20025–20032.
636 Salter, S. J., M. J. Cox, E. M. Turek, S. T. Calus, W. O. Cookson, M. F. Moffatt, P. Turner, J.
637 Parkhill, N. J. Loman, and A. W. Walker. (2014). Reagent and laboratory contamination
638 can critically impact sequence-based microbiome analyses. *BMC Biology*, 12, 87.
639 Springer.
640 Santos-Garcia, D., F. J. Silva, S. Morin, K. Dettner, and S. M. Kuechler. (2017). The All-
641 Rounder Sodalis: A New Bacteriome-Associated Endosymbiont of the Lygaeoid Bug
642 Henestaris halophilus (Heteroptera: Henestarinae) and a Critical Examination of Its
643 Evolution. *Genome Biology and Evolution*, 9, 2893–2910.

644 Slowikowski, K., A. Schep, S. Hughes, S. Lukauskas, J. O. Irisson, and Z. N. Kamvar. (2019).
645 ggrepel: automatically position non-overlapping text labels with 'ggplot2'2018. URL
646 https://CRAN. R-project. org/package= ggrepel. R package version 0.8. 0.
647 Snodgrass, R. E. (1944). The feeding apparatus of biting and sucking insects affecting man and
648 animals. Smithsonian Miscellaneous Collections.
649 Song, S. J., J. G. Sanders, F. Delsuc, J. Metcalf, K. Amato, M. W. Taylor, F. Mazel, H. L. Lutz,
650 K. Winker, G. R. Graves, G. Humphrey, J. A. Gilbert, S. J. Hackett, K. P. White, H. R.
651 Skeen, S. M. Kurtis, J. Withrow, T. Braile, M. Miller, K. G. McCracken, J. M. Maley, V.
652 O. Ezenwa, A. Williams, J. M. Blanton, V. J. McKenzie, and R. Knight. (2020).
653 Comparative Analyses of Vertebrate Gut Microbiomes Reveal Convergence between
654 Birds and Bats. *mBio*, 11.
655 Souza, A. V. G., J. H. Petretski, M. Demasi, E. J. H. Bechara, and P. L. Oliveira. (1997). Urate
656 protects a blood-sucking insect against hemin-induced oxidative stress. *Free Radical*
657 *Biology & Medicine*, 22, 209–214.
658 Suzuki, T. A., M. Phifer-Rixey, K. L. Mack, M. J. Sheehan, D. Lin, K. Bi, and M. W. Nachman.
659 (2019). Host genetic determinants of the gut microbiota of wild mice. *Molecular*
660 *Ecology*, 28, 3197–3207.
661 Swei, A., and J. Y. Kwan. (2017). Tick microbiome and pathogen acquisition altered by host
662 blood meal. *ISME Journal*, 11, 813–816.
663 Terra, W. R. (2001). The origin and functions of the insect peritrophic membrane and peritrophic
664 gel. *Archives of Insect Biochemistry and Physiology*, 47, 47–61.
665 Uritskiy, G. V., J. DiRuggiero, and J. Taylor. (2018). MetaWRAP—a flexible pipeline for
666 genome-resolved metagenomic data analysis. *Microbiome,* 6, 158.
667 Velazquez, E. M., H. Nguyen, K. T. Heasley, C. H. Saechao, L. M. Gil, A. W. L. Rogers, B. M.
668 Miller, M. R. Rolston, C. A. Lopez, Y. Litvak, M. J. Liou, F. Faber, D. N. Bronner, C. R.
669 Tiffany, M. X. Byndloss, A. J. Byndloss, and A. J. Bäumler. (2019). Endogenous
670 Enterobacteriaceae underlie variation in susceptibility to Salmonella infection. *Nature*
671 *Microbiology*, 4, 1057–1064.
672 Wang, Y., T. M. G. Iii, P. Kukutla, G. Yan, and J. Xu. (2011). Dynamic Gut Microbiome across
673 Life History of the Malaria Mosquito Anopheles gambiae in Kenya. *PloS One*, 6, e24767.
674 Waniek, P. J. (2009). The digestive system of human lice: current advances and potential
675 applications. *Physiological Entomology*, 34, 203–210.
676 Weiss, S., Z. Z. Xu, S. Peddada, A. Amir, K. Bittinger, A. Gonzalez, C. Lozupone, J. R.
677 Zaneveld, Y. Vázquez-Baeza, A. Birmingham, E. R. Hyde, and R. Knight. (2017).
678 Normalization and microbial differential abundance strategies depend upon data
679 characteristics. *Microbiome*, 5, 27.
680 Wernegreen, J. J. (2015). Endosymbiont evolution: Predictions from theory and surprises from
681 genomes. *Annals of the New York Academy of Sciences*, 1360, 16–35.
682 Werren, J. H. (1997). Biology of wolbachia. *Annual Review of Entomology*, 42, 587–609.
683 Wickham, H. (2016). ggplot2: elegant graphics for data analysis. Springer.
684 Willner, D., J. Daly, D. Whiley, K. Grimwood, C. E. Wainwright, and P. Hugenholtz. (2012).
685 Comparison of DNA extraction methods for microbial community profiling with an
686 application to pediatric bronchoalveolar lavage samples. *PloS One*, 7.
687 Wu, Y.-W., B. A. Simmons, and S. W. Singer. (2016). MaxBin 2.0: an automated binning
688 algorithm to recover genomes from multiple metagenomic datasets. *Bioinformatics,* 32,
689 605–607.

690 Xiao, N. (2018). ggsci: scientific journal and sci-fi themed color palettes for 'ggplot2'. R
691 package version 2.9.
692 Zhang, X.-C., Z.-N. Yang, B. Lu, X.-F. Ma, C.-X. Zhang, and H.-J. Xu. (2014). The composition
693 and transmission of microbiome in hard tick, Ixodes persulcatus, during blood meal.
694 *Ticks and Tick-Borne Diseases*, 5, 864–870.
695 Zolnik, C. P., R. C. Falco, T. J. Daniels, and S.-O. Kolokotronis. (2018). Transient influence of
696 blood meal and natural environment on blacklegged tick bacterial communities. *Ticks*
697 *and Tick-Borne Diseases*, 9, 563–572.
698

699 **Figure and table legend:**

700 **Table 1.** Statistics of the MAGs assembled. MAG name indicates the name given to that bin for
701 this study (e.g., in Figure 1). The highest taxonomic rank with p-value ≤ 0.5 is shown in MiGA
702 ID. RPD ID is the result of the identification analysis using rRNA genes (16S) implemented in
703 MiGA; % indicates confidence in identification. Taxonomic novelty is a MiGA analysis that
704 indicates the taxonomic rank at which the MAG represents a novel taxon with respect to the NCBI
705 Genome database; highest taxonomic rank with p-value ≤ 0.01 are shown.

MAG name	Completeness (%)	Contamination (%)	N50 (bp)	Size (bp)	Taxator tk ID	MiGA ID	RDP ID	Taxonomic novelty
bin.1	100	1.07	57370	1869975	Flavobacteriaceae	Flavobacteriaceae*	NA	Species****
bin.4	99.26	0.24	81315	2500734	Flavobacteriaceae	Chryseobacterium*	Chryseobacterium (100.0%)	Species****
bin.2	98.51	0.42	36844	3101576	Deinococcus	Deinococcus grandis*	Deinococcus (100.0%)	Subspecies****
bin.7	97.75	0	16123	2650064	Moraxellaceae	Psychrobacter sp. PRwf-1*	NA	Subspecies****
bin.3	97.41	1.33	32961	4014303	Neisseriales	Pseudogulbenkiania*	NA	Species****
bin.11	95.65	0.92	69243	2786419	Moraxellaceae	Psychrobacter*	NA	Species****
bin.10	95.12	0	13409	2459723	Deinococcaceae	Deinococcus*	NA	Species****
bin.12	93.14	0.85	24793	2851493	Deinococcaceae	Deinococcus*	NA	Species****
bin.6	88.74	1.45	7283	1988194	Micrococcales	Arthrobacter*	NA	Species****
bin.13	77.11	0.64	3045	2627969	Deinococcaceae	Deinococcus*	NA	Species****
bin.5	74.13	0.61	24837	1635952	Moraxellaceae	unclassified Moraxellaceae*	Alkanindiges (99 %)	Species****
bin.8	67.76	0	10934	2837743	Deinococcaceae	Deinococcus*	NA	Species****

bin.9	61.13	0.30	2210	2110411	Janthinobacterium	Janthinobacterium sp. SNU WT3***	NA	Subspecies****

Significance at p-value below: *0.5, **0.1, ***0.05, ****0.01

Figure 1. Genome-resolved metagenomic data. a) Stacked bar plot showing the relative abundances of MAGs in each louse sample. Note that samples are ordered according to host (i.e., samples from the same host are next to each other). b) Boxplot summarizing the relative abundance of each MAG across the louse samples.

/

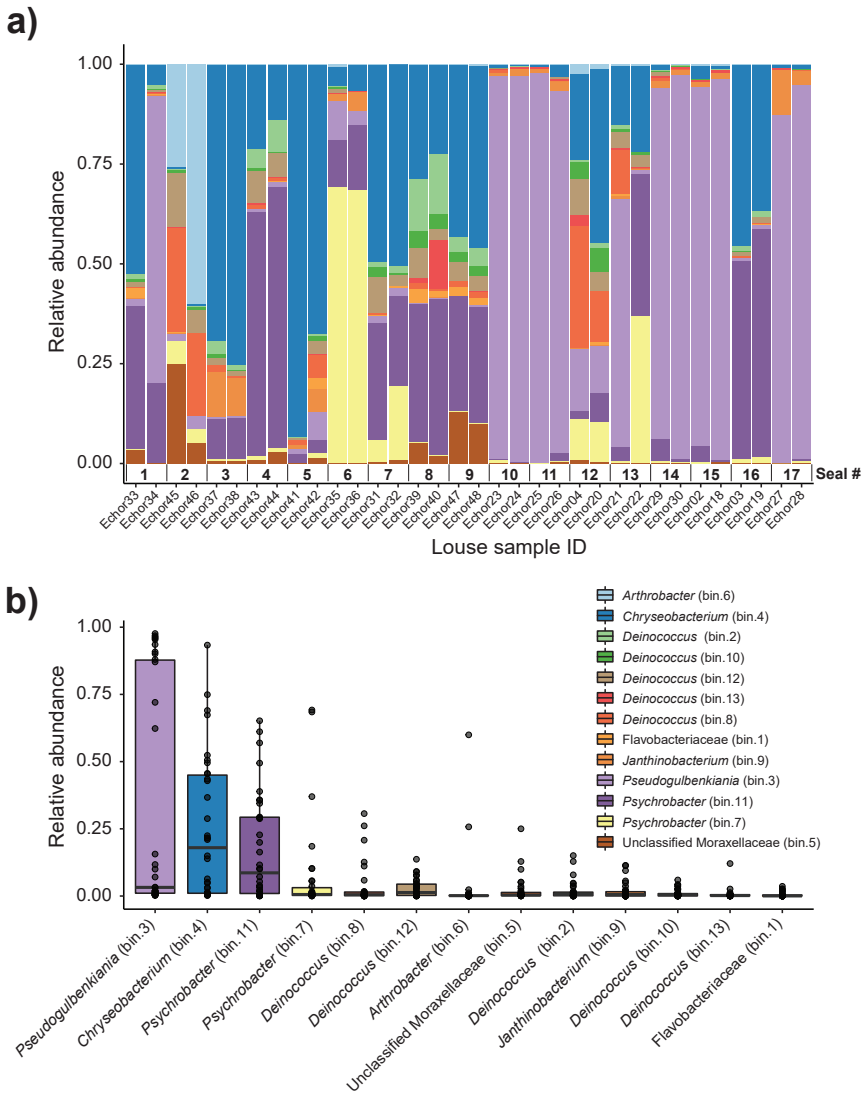

Figure 2. Kaiju data. a) Stacked bar plot showing bacterial relative abundances in each seal louse sample. Note that samples are sorted according to host individual (i.e., samples from the same host are next to each other). b) Boxplot summarizing the relative abundance of each taxon across all louse samples.

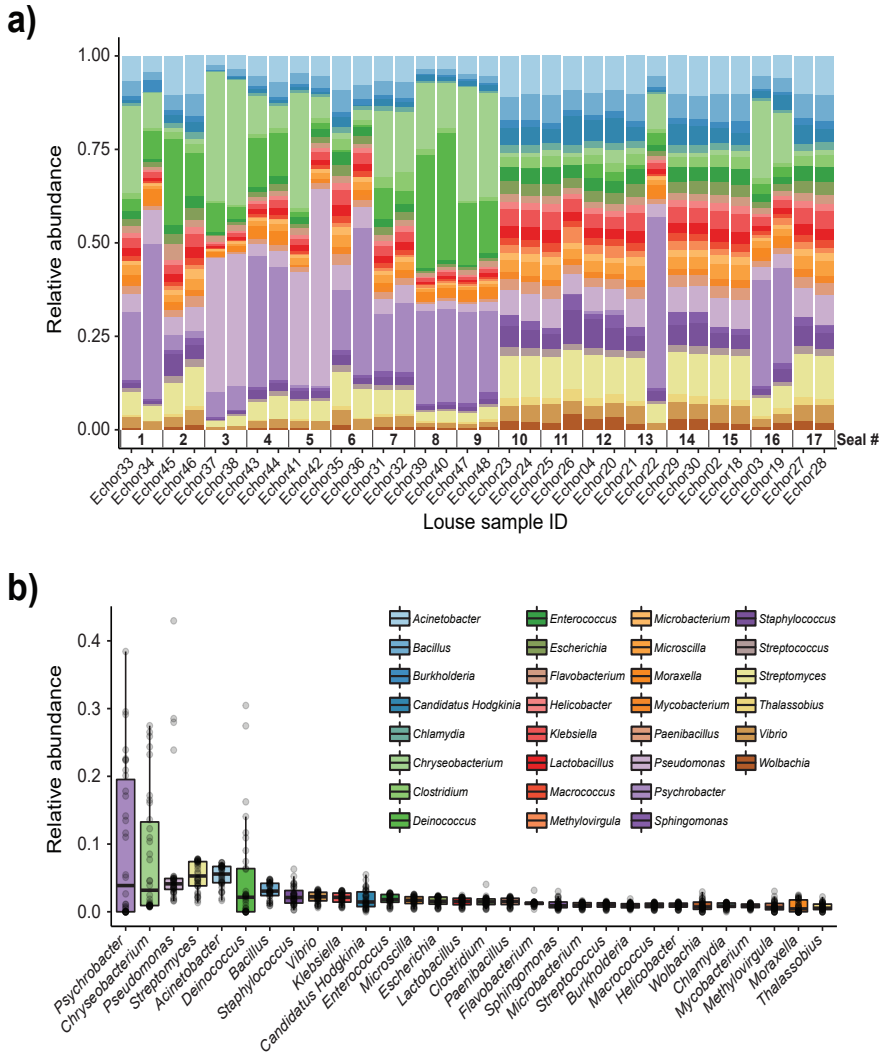

/

720 **Figure 3.** NMDS ordinations of seal louse microbiomes base on Bray–Curtis dissimilarity
721 matrices. a) MAG matrix, and b) Kaiju matrix (species level). Lice originating from the same
722 seal individual are colored similarly and connected by a line.
723 /

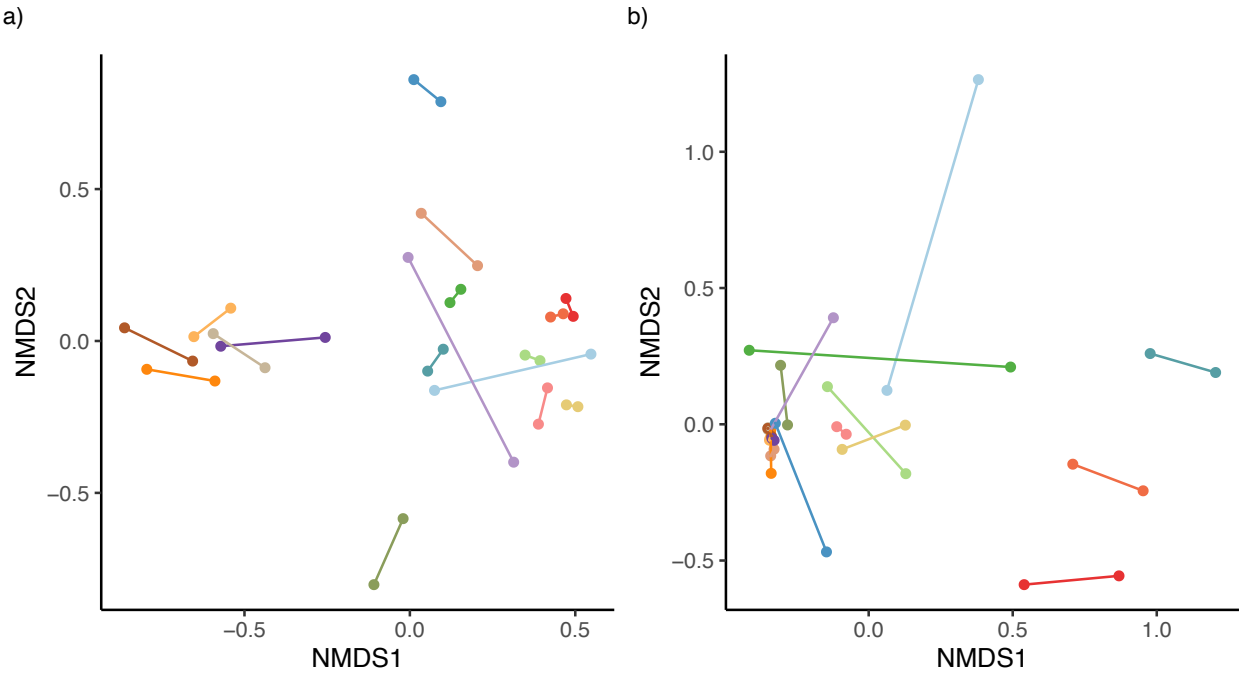

724

725 **Figure 4.** Scatter plot showing the relationship between genome size (Mb) and GC content (i.e.,
726 proportion of G and C sites) for sequenced MAGs.

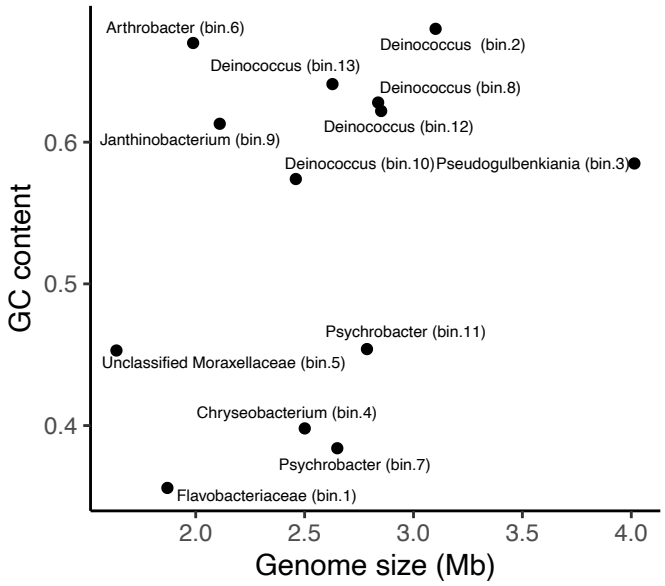

727 /
728

729